# A second order numerical scheme for optimal control of non-linear Fokker–Planck equations and applications in social dynamics

G. Albi\* E. Calzola <sup>†</sup>

March 14, 2025

#### Abstract

In this work, we present a second-order numerical scheme to address the solution of optimal control problems constrained by the evolution of nonlinear Fokker–Planck equations arising from socio—economic dynamics. In order to design an appropriate numerical scheme for control realization, a coupled forward-backward system is derived based on the associated optimality conditions. The forward equation, corresponding to the Fokker–Planck dynamics, is discretized using a structure preserving scheme able to capture steady states. On the other hand, the backward equation, modeled as a Hamilton–Jacobi–Bellman problem, is solved via a semi-Lagrangian scheme that supports large time steps while preserving stability. Coupling between the forward and backward problems is achieved through a gradient descent optimization strategy, ensuring convergence to the optimal control. Numerical experiments demonstrate second-order accuracy, computational efficiency, and effectiveness in controlling different examples across various scenarios in social dynamics. This approach provides a reliable computational tool for the study of opinion manipulation and consensus formation in socially structured systems.

**Keywords:** Optimal control, Fokker–Planck equation, Hamilton–Jacobi equation, Opinion dynamics.

MSC codes: 35Q84, 49L12, 91D30, 65N08, 65M25

#### Contents

1	Introduction	2
2	Optimal control of non-local Fokker–Planck equations	3
3	Discretization of the optimality system	5
	3.1 The second order semi-Lagrangian scheme for the backward equation	5
	3.2 The structure preserving scheme for the forward Fokker–Planck equation $\dots$	7
-	*Department of Computer Science, University of Verona, Strada le Grazie 15, 37134 Verona, Italy.	(gia-

como.albi@univr.it)

†Department of Computer Science, University of Verona, Strada le Grazie 15, 37134 Verona, Italy.
(elisa.calzola@univr.it)

4 Numerical simulations				
	4.1	Convergence to the stationary state for the Fokker–Planck	9	
	4.2	Order check with fixed suboptimal control for the Hamilton–Jacobi equation	9	
4.3 Numerical experiments in social dynamics				
		4.3.1 Evolving opinions and social media contacts	12	
		4.3.2 Bivariate opinion model	14	
5	Cor	nelusions	16	

#### 1 Introduction

In this manuscript we focus on the development of numerical methods for optimal control problems constrained by the evolution of a nonlinear Fokker–Planck equation of the form

$$\partial_t f = -\nabla \cdot (\mathcal{G}[f; \mathbf{u}](\mathbf{v}, t)f - \nabla \cdot (\mathcal{D}(\mathbf{v})f)), \qquad (1.1)$$

where  $\mathbf{v} \in \Omega \subseteq \mathbb{R}^d$ ,  $f(\mathbf{v}, t) \geq 0$  and  $t \geq 0$ , and where the control  $\mathbf{u}(\mathbf{v}, t) \in \mathbb{R}^d$  is solution to the following objective functional

$$\mathbf{u} = \arg\min_{\mathbf{u} \in U} \mathcal{J}(\mathbf{u}; f_0). \tag{1.2}$$

In particular, we aim at describing dynamics where  $f(\mathbf{v}, t)$  represents a continuous population, the controlled non-linear drift  $\mathcal{G}[\cdot]$  encodes non-local interactions among the agents' population, and the non-linear function  $\mathcal{D}(\cdot) \geq 0$  weights the influence of the diffusion.

Fokker–Planck models of type (1.1) arise in several fields of applications such as in plasma physics [13], in biology [23, 25], in socio-economic dynamics [39, 26, 36], as well as optimization and learning methods [22, 30]. The study of the nonlinear optimization problem constrained by PDEs (1.1)-(1.2) is motivated by the need to design efficient control strategies in these different areas of application domains. In particular in the last decade large interest has been shown in the context of control of multi-agent systems at various scales, see for example [6, 19, 32, 33, 5, 31]. In particular, the optimal control of Fokker–Planck models has been studied in several directions, for example in [11, 29] from a theoretical perspectives, or in a stochastic setting in [18, 10], as well as stabilization problems [17, 12, 9]. In this framework, the numerical realization of the control requires careful treatment because of nonlinearities involved that must be treated efficiently to achieve solutions with proper accuracy and within a reasonable computational time, see for example [2, 5, 3, 1]. Here we address the control synthesis by means of reduced gradient method, solving the associated optimality conditions. This approach results in solving numerically the coupled system of the Fokker–Planck model and the associated backward equation, see for instance [5].

Hence, the forward problem, corresponding to the evolution of the Fokker-Planck equation, is approximated with a Chang-Cooper scheme [24, 35], where in this case for the non-linear drift we follow the approach proposed in [37]. The backward equation is modeled as a Hamilton-Jacobi-Bellman problem, for which we use a semi-Lagrangian scheme that supports large time steps while preserving stability [27, 21, 8]. Unlike standard Eulerian approaches, semi-Lagrangian schemes handle naturally the presence of advection and diffusion terms and are explicit and stable without requiring any parabolic CFL condition, thus proving to be flexible tools for complex problems. These methods can achieve high order of accuracy thanks to the choice of appropriate interpolation techniques and, in the viscous case, by implementing different treatments of the diffusion terms [28].

Moreover their implementation adapts well also to various domain geometries and can be made efficient on unstructured meshes [20]. Eventually, in order to optimize the cost (1.2), the forward and backward equations are coupled through an iterative reduced-gradient descent procedure, to provide the optimal control solution. Similar approaches for mean-field optimal control problem, such as (1.1)–(1.2) have been studied in [5, 1, 16], here the main novelty consists in deriving a second order scheme both for the forward and backward equation, in order to gain accuracy in the solution, as well providing different numerical experiments in a multi-dimensional setting for some collective dynamics, such as evolution of opinions [7, 39, 4].

The manuscript is structured as follows. Section 2 presents the PDE constrained optimization problem, and shows how to derive a forward-backward system of coupled equations and the optimality conditions for the control function. A gradient descent approach is presented to approximate such optimality conditions in Section 3, and introduces the combination of numerical schemes used to approximate the solution of the optimality conditions. In particular, Section 3.1 introduces the second order semi-Lagrangian discretization for the Hamilton-Jacobi equation, while Section 3.2 presents the second order structure preserving scheme for the Fokker-Planck equation. Both schemes do not require a parabolic CFL condition for stability, allowing for the use of larger time steps, which is crucial when an unknown number of iterations of the gradient descent approach are necessary to reach the optimality condition. Finally, Section 4 presents some numerical simulations, in particular Section 4.1 shows the order two of convergence of the structure preserving scheme to the stationary solution of the Fokker-Planck equation, while Section 4.2 is dedicated to showing the order two of convergence of the coupled two methods for the forward-backward system, given a fixed suboptimal control. Finally, Section 4.3 presents applications in social dynamics in two spatial dimensions: Section 4.3.1 presents a model in which the first variable is the opinion on a given topic and the second one is the number of social media contacts, modeling the controlled process of opinion evolution on an evolving social network, while Section 4.3.2 is dedicated to a two-opinions model, where the controlled evolution of two opinions (that influence each other) is studied. Section 5 presents some concluding remarks and possible future research directions.

## 2 Optimal control of non-local Fokker-Planck equations

Let  $\mathbf{v} = (v_1, \dots, v_d) \in \Omega \subset \mathbb{R}^d$ . Given T > 0, we will use the notation  $\Omega_T = \Omega \times (0, T]$  for the spatiotemporal domain and  $\vec{n}(\mathbf{v})$  to indicate the outward pointing normal vector in any point  $\mathbf{v} \in \partial \Omega$ . We want to numerically solve the mean-field optimal control problem

$$\min_{\mathbf{u} \in U} \mathcal{J}(\mathbf{u}; f_0) \tag{2.3}$$

under the conditions

$$\begin{cases}
\partial_t f = -\nabla \cdot (\mathcal{G}[f; \mathbf{u}](\mathbf{v}, t) f - \nabla \cdot (\mathcal{D}(\mathbf{v}) f)), & (\mathbf{v}, t) \in \Omega_T \\
f(\mathbf{v}, 0) = f_0(\mathbf{v}), & \mathbf{v} \in \Omega \\
(-\mathcal{G}[f, \mathbf{u}](\mathbf{v}, t) f + \nabla (\mathcal{D}(\mathbf{v}) f)) \cdot \vec{n}(\mathbf{v}) = 0, & \mathbf{v} \in \partial \Omega,
\end{cases}$$
(2.4)

where the drift  $\mathcal{G}$  depends on the control  $\mathbf{u} = (u_1, \dots, u_d) \in U$  and is defined as

$$G[f; \mathbf{u}](\mathbf{v}, t) = P[f](\mathbf{v}, t) + \mathbf{u}(\mathbf{v}, t), \tag{2.5}$$

where  $\mathcal{P}[f](\mathbf{v},t)$  is a vector whose components are the operators  $\mathcal{P}_i[f]$ , that can be expressed as the sum of a local and a nonlocal term. For  $i=1,\ldots,d$  we have

$$\mathcal{P}_i[f](\mathbf{v},t) = h_i(\mathbf{v}) + \int_{\Omega} \alpha_i P_i(\mathbf{v}, \mathbf{v}^*) (v_i^* - v_i) f(\mathbf{v}^*, t) d\mathbf{v}^*, \tag{2.6}$$

with  $h_i(\mathbf{v})$  a given function,  $\alpha_i \in [0, 0.5]$  and  $P_i$  a given interaction function. The diffusion is given by the matrix

$$\mathcal{D}(\mathbf{v}) = \operatorname{diag}(D_1(\mathbf{v}), \dots, D_d(\mathbf{v})). \tag{2.7}$$

The cost functional  $\mathcal{J}$  is defined as

$$\mathcal{J}(\mathbf{u}; f_0) = \frac{1}{2} \int_0^T \int_{\Omega} \left( \sum_{i=1}^d |v_i - \overline{v}_i|^2 s_i(\mathbf{v}) + \gamma ||\mathbf{u}||^2 \right) f(\mathbf{v}, t) d\mathbf{v} dt,$$
 (2.8)

where  $\|\cdot\|$  indicates the Euclidean norm. The solution  $f(\mathbf{v},t)$  of the constraint function in (2.4) must be understood as a probability density, which means that

$$\int_{\Omega} f(\mathbf{v}, t) d\mathbf{v} = 1 \quad \text{for all } t \in [0, T].$$

In order to solve problem (2.3)-(2.4) we resort to the Lagrangian approach ([5, 19, 34]), so we introduce the Lagrangian function

$$\mathcal{L}(f, \mathbf{u}, \psi) = \mathcal{J}(\mathbf{u}; f_0)$$

$$- \int_0^T \int_{\Omega} \psi \left( \partial_t f + \nabla \cdot (\mathcal{G}[f; \mathbf{u}](\mathbf{v}, t) f - \nabla \cdot (\mathcal{D}(\mathbf{v}) f)) \right) d\mathbf{v} dt.$$

Hence, we derive the optimality conditions by computing the Fréchet derivatives of the Lagrangian, meaning that we want to numerically solve

$$\begin{cases}
D_f \mathcal{L}(f, \mathbf{u}, \psi) = 0, \\
D_{\mathbf{u}} \mathcal{L}(f, \mathbf{u}, \psi) = 0, \\
D_{\psi} \mathcal{L}(f, \mathbf{u}, \psi) = 0.
\end{cases}$$
(2.9)

The first equation in (2.9) results in the adjoint backward equation

$$-\partial_t \psi = \mathcal{G}[f; \mathbf{u}](\mathbf{v}, t) \cdot \nabla \psi + (\mathcal{D}(\mathbf{v}) \nabla^\top) \cdot \nabla \psi + \sum_{i=1}^d \mathcal{Q}_i[f, \psi](\mathbf{v}, t) + \frac{1}{2} \left( \sum_{i=1}^d |v_i - \overline{v}_i|^2 s_i(\mathbf{v}) + \gamma ||\mathbf{u}||^2 \right),$$
(2.10)

where the nonlocal operators  $Q_i[f, \psi]$ , i = 1, ..., n, are defined as

$$Q_i[f, \psi](\mathbf{v}, t) = \int_{\Omega} \alpha_i P_i(\mathbf{v}^*, \mathbf{v})(v_i - v_i^*) f(\mathbf{v}^*, t) \partial_{v_i} \psi(\mathbf{v}^*, t) d\mathbf{v}^*,$$

the second equation gives the optimality condition

$$\gamma \mathbf{u}(\mathbf{v}, t) + \nabla \psi(\mathbf{v}, t) = 0 \tag{2.11}$$

and the third one corresponds to the Fokker-Planck equation (2.4).

In the following section we will detail the derivation of the numerical schemes involved, as well as their properties for the current optimal control problem.

## 3 Discretization of the optimality system

In order to find a candidate solution for the optimality condition system (2.9) we will proceed numerically using a reduced-gradient method. Hence, starting from  $\mathbf{u}^{(0)} = \mathbf{0}$  and an initial guess for the density  $f = f^{(0)}$ , we aim to approach iteratively the solution of (2.3)-(2.4). At each iteration k we approximate the solution to the forward problem (2.4) with a semi-implicit structure preserving scheme, in order to obtain the  $f^{(k)}$  over the whole time frame [0, T]. Subsequently,  $f^{(k)}$  is passed in the backward equation (2.10), where its solution  $\psi^{(k)}$  is discretized with a semi-Lagrangian scheme. Then we perform a gradient descent step to update the control variable

$$\mathbf{u}^{(k)} = \mathbf{u}^{(k-1)} - \lambda D_{\mathbf{u}}(f^{(k-1)}, \mathbf{u}^{(k-1)}, \psi^{(k)}),$$

and we will iterate the process until we reach the minimum of (2.8).

In the sequel, we will focus on the two-dimensional case in order to make the notation easier to read, but everything can be extended to a general d-dimensional framework. Let  $\Omega = \Omega_1 \times \Omega_2$ , with  $\Omega_1$  and  $\Omega_2$  compact connected subsets of  $\mathbb{R}$ . We choose two discretization steps,  $\Delta v_1, \Delta v_2 > 0$ , and since we can rewrite  $\Omega_1 = [a_1, b_1]$  and  $\Omega_2 = [a_2, b_2]$  we define the grid

$$G_{\Delta v_1, \Delta v_2} = \{ \mathbf{v}_{i,j} = (v_{1,i}, v_{2,j}) \text{ s.t. for } k = 1, 2$$

$$v_{k,i} = a_1 + \Delta v_k (i + 1/2), i = 0, \dots, N_{v_k} - 1 \},$$
(3.12)

where  $N_{v_1}=|\Omega_1|/\Delta v_1$  and  $N_{v_2}=|\Omega_2|/\Delta v_2$ . We also fix a time discretization step  $\Delta t>0$ , a number of time steps  $N_t=T/\Delta t$ , such that  $t^n=n\Delta t,\,n=0,\ldots,N_t$ . Concerning the choice of  $\Delta t$ , both the semi-Lagrangian scheme and the semi-implicit structure preserving one do not require a parabolic CFL condition in order to ensure stability, meaning that we can set the same time step for both methods equal to  $\Delta t=\Delta v_1\Delta v_2/(K(\Delta v_1+\Delta v_2))$ , for some constant K>0 such that positivity of the solution of the scheme for (2.4) is preserved. We will use the notation  $\psi_{i,j}^n$  and  $f_{ij}^n$  to indicate the numerical approximation of  $\psi$  and f in  $\mathbf{v}_{i,j}\in G_{\Delta v_1,\Delta v_2}$  at time  $t^n$ , and we will indicate with  $\boldsymbol{\psi}^n=(\psi_{i,j}^n)_{i,j}$  and  $\mathbf{f}^n=(f_{i,j}^n)_{i,j}$  the set of all their values on  $G_{\Delta v_1,\Delta v_2}$ .

# 3.1 The second order semi-Lagrangian scheme for the backward equation

Considering f,  $\mathbf{u}$  two given functions, we can write the second order in time and space semi-Lagrangian approximation of (2.10) as in, for example, [14]. On the uniform grid  $G_{\Delta v_1,\Delta v_2}$  it is possible to define  $\mathbb{I}^r$ , a piecewise polynomial interpolation operator of order r constructed on the values of a grid function  $\mathbf{g}$  such that  $\mathbb{I}^r[\mathbf{g}](\mathbf{v}_{i,j}) = g_{i,j}$ . Let  $K = [v_{1,i}, v_{1,i+1}] \times [v_{2,j}, v_{2,j+1}]$  be an element of the discretization defined in (3.12), then for all  $g \in C^{r+1}(K)$ ,  $g(\mathbf{v}_{i,j}) = g_{i,j}$ , the following local error estimate holds

$$||g - \mathbb{I}^r[\mathbf{g}]||_{L^2(K)} \le C \left( \max\{\Delta v_1, \Delta v_2\} \right)^{r+1},$$

for a suitable constant C > 0, leading to the global estimate

$$||g - \mathbb{I}^r[\mathbf{g}]||_{L^2(\Omega_1 \times \Omega_2)} \le C \left( \max\{\Delta v_1, \Delta v_2\} \right)^{r+1},$$

if we also have  $g \in H^{r+1}(\Omega)$  (we refer to [38, Chapter 4.5] for a proof). In our simulations, we set r = 3, in order to keep the interpolation error lower than the error due to the approximation of the stochastic characteristics.

Defining  $\mathbf{V} = (V_1, V_2)$ , for  $s \in [t, t + \Delta t]$  the characteristic curves for equation (2.10) solve the following SDE

$$\begin{cases} d\mathbf{V} = \mathcal{G}[f; \mathbf{u}](\mathbf{V}(s), s) ds + \sqrt{2\mathcal{D}(\mathbf{V}(s))} d\mathbf{W}(s), \\ \mathbf{V}(t + \Delta t) = \mathbf{v}, \end{cases}$$
(3.13)

where **W** is a standard two-dimensional Brownian motion. At each time step  $t^n$  the second order numerical approximation of the characteristic curves (3.13) is given by  $(y_{i,j}^{n,\ell})$ ,  $\ell=1,\ldots,9$ , where

$$y_{i,j}^{n,\ell} = \mathbf{v}_{i,j} + \frac{\Delta t}{2} \left( \mathcal{G}[\mathbf{f}^n; \mathbf{u}^n](\mathbf{v}_{i,j}, t^n) + \mathbb{I}^r [\mathcal{V}[\mathbf{f}^{n+1}; \mathbf{u}^{n+1}]](y_{i,j}^{n,\ell}) \right) + \sqrt{2\Delta t \mathcal{D}(\mathbf{v}_{i,j})} \mathbf{e}^{\ell},$$
(3.14)

and the vectors  $\mathbf{e}^{\ell}$ ,  $\ell = 1, \dots, 9$  are defined as

$$\mathbf{e}^{1} = \begin{bmatrix} 0 \\ 0 \end{bmatrix}, \qquad \mathbf{e}^{2} = \begin{bmatrix} +\sqrt{3} \\ 0 \end{bmatrix}, \quad \mathbf{e}^{3} = \begin{bmatrix} -\sqrt{3} \\ 0 \end{bmatrix},$$

$$\mathbf{e}^{4} = \begin{bmatrix} 0 \\ +\sqrt{3} \end{bmatrix}, \qquad \mathbf{e}^{5} = \begin{bmatrix} 0 \\ -\sqrt{3} \end{bmatrix}, \quad \mathbf{e}^{6} = \begin{bmatrix} +\sqrt{3} \\ +\sqrt{3} \end{bmatrix},$$

$$\mathbf{e}^{7} = \begin{bmatrix} -\sqrt{3} \\ +\sqrt{3} \end{bmatrix}, \qquad \mathbf{e}^{8} = \begin{bmatrix} +\sqrt{3} \\ -\sqrt{3} \end{bmatrix}, \quad \mathbf{e}^{9} = \begin{bmatrix} -\sqrt{3} \\ -\sqrt{3} \end{bmatrix}.$$

For what concerns the treatment of the homogeneous Neumann boundary conditions we use the same approach presented in [21]. For  $y \notin \Omega_1 \times \Omega_2$  we define  $\pi^{\vec{n}}(\cdot)$ , the projection operator along the direction  $\vec{n}$  orthogonal to the boundary  $\partial (\Omega_1 \times \Omega_2)$ . Whenever a characteristic curve  $y_{i,j}^{n,\ell}$ , for some values of i, j, n and  $\ell$ , falls out of the domain, we reflect it inside in the point

$$\pi^{\vec{n}}(y_{i,j}^{n,\ell}) - \overline{c}\sqrt{\Delta t}\vec{n}(\pi^{\vec{n}}(y_{i,j}^{n,\ell}))$$

where  $\bar{c} > 0$  is a fixed constant. This leads to the modified definition of the characteristic curves

$$\tilde{y}_{i,j}^{n,\ell} = \begin{cases} y_{i,j}^{n,\ell}, & \text{if } y_{i,j}^{n,\ell} \in \Omega_1 \times \Omega_2, \\ \pi^{\vec{n}}(y_{i,j}^{n,\ell}) - \overline{c}\sqrt{\Delta t}\vec{n}(\pi^{\vec{n}}(y_{i,j}^{n,\ell})), & \text{if } y_{i,j}^{n,\ell} \notin \Omega_1 \times \Omega_2. \end{cases}$$
(3.15)

We introduce the following notation for the reaction term in (2.10)

$$\mathcal{R}[f, \psi, \mathbf{u}](\mathbf{v}, t) = \mathcal{Q}_1[f, \psi](\mathbf{v}, t) + \mathcal{Q}_2[f, \psi](\mathbf{v}, t)$$
$$+ \frac{1}{2} \left( |v_1 - \overline{v}_1|^2 s_1(v) + |v_2 - \overline{v}_2|^2 s_2(v) + \gamma ||\mathbf{u}||^2 \right),$$

so that the scheme for the backward equation reads as

$$\psi_{i,j}^{n} = \sum_{\ell=1}^{9} \omega^{\ell} \left( \mathbb{I}^{r} [\boldsymbol{\psi}^{n+1}] \left( \tilde{y}_{i,j}^{n,\ell} \right) + \frac{\Delta t}{2} \mathbb{I}^{r} \left[ \mathcal{R} [\mathbf{f}^{n+1}, \boldsymbol{\psi}^{n+1}, \mathbf{u}^{n+1}] \right] (\tilde{y}_{i,j}^{n,\ell}) \right)$$

$$+ \frac{\Delta t}{2} \mathcal{R} [\mathbf{f}^{n}, \boldsymbol{\psi}^{n}, \mathbf{u}^{n}] (\mathbf{v}_{i,j}, t^{n}),$$
(3.16)

for all  $n = 0, ..., N_t - 1$  and with  $\omega^1 = 4/9$ ,  $\omega^2 = \omega^3 = \omega^4 = \omega^5 = 1/9$ ,  $\omega^6 = \omega^7 = \omega^8 = \omega^9 = 1/36$ . Since we are dealing with homogeneous Neumann boundary conditions, the correction term appearing in the scheme described in [21] is equal to zero and the only modification we make to a classical second order semi-Lagrangian discretization consists in the use of the reflected characteristic defined in (3.15).

# 3.2 The structure preserving scheme for the forward Fokker–Planck equation

For the forward equation in (2.4) we apply the structure preserving scheme in [37], which is in practice a Chang-Cooper type of scheme. In order to take advantage of the fact that the semi-Lagrangian scheme used for (2.10) does not have a parabolic CFL condition, we implemented a semi-implicit version of such scheme. We choose the same discretization steps  $\Delta v_1, \Delta v_2$  and  $\Delta t$  that we used for the semi-Lagrangian scheme. We rewrite equation (2.4) in divergence form

$$\partial_t f = \nabla \cdot \mathcal{F}[f, u](v_1, v_2, t), \tag{3.17}$$

with

$$\mathcal{F}[f, u](v_1, v_2, t) = (-\mathcal{G}[f; u](v_i, v_2, t) + \nabla \cdot \mathcal{D}(v_1, v_2)) f + \mathcal{D}(v_1, v_2) \nabla f$$
(3.18)

Using the uniform spatial grid previously introduced, we denote with  $v_{1,i\pm\frac{1}{2}}=v_{1,i}\pm\Delta v_1/2$  and  $v_{2,j\pm\frac{1}{2}}=v_{2,j}+\Delta v_2/2$ . Supposing the control **u** to be given, we use the notation  $\mathcal{F}_{i,j}^{(1)}$  and  $\mathcal{F}_{i,j}^{(2)}$ , respectively, for the first and the second component of the flux (3.18) in  $\mathbf{v}_{i,j}$ . We consider the semi-discrete approximation

$$\frac{\mathrm{d}}{\mathrm{d}t}f_{i,j}(t) = \frac{\mathcal{F}_{i+\frac{1}{2},j}^{(1)}(t) - \mathcal{F}_{i-\frac{1}{2},j}^{(1)}(t)}{\Delta v_1} + \frac{\mathcal{F}_{i,j+\frac{1}{2}}^{(2)}(t) - \mathcal{F}_{i,j-\frac{1}{2}}^{(2)}(t)}{\Delta v_2},\tag{3.19}$$

for all  $t \geq 0$ , where  $\mathbf{f} = (f_{i,j})_{i,j}$ ,  $f_{i,j}(t)$  approximates  $f(v_i, c_j, t)$ ,  $\mathcal{F}^{(1)}_{i \pm \frac{1}{2}, j}$  is the numerical flux along the first axis, while  $\mathcal{F}^{(2)}_{i,j \pm \frac{1}{2}}$  is the numerical flux along the second axis. Defining  $\mathcal{A}[f; \mathbf{u}](v_1, v_2, t) = -\mathcal{P}_1[f](v_1, v_2, t) - u_1(v_1, v_2, t) + \partial_{v_1} D_1(v_1, v_2)$  and  $\mathcal{B}[f; \mathbf{u}](v_1, v_2, t) = -\mathcal{P}_2[f; u](v_1, v_2, t) - u_2(v_1, v_2, t) + \partial_{v_2} D_2(v_1, v_2)$ , we consider the fluxes

$$\mathcal{F}_{i+\frac{1}{2},j}^{(1)} = \mathcal{A}_{i+\frac{1}{2},j} \tilde{f}_{i+\frac{1}{2},j} + D_1(v_{i+\frac{1}{2},j}) \frac{f_{i+1,j} - f_{i,j}}{\Delta v_1}, 
\mathcal{F}_{i,j+\frac{1}{2}}^{(2)} = \mathcal{B}_{i,j+\frac{1}{2}} \tilde{f}_{i,j+\frac{1}{2}} + D_2(v_{i,j+\frac{1}{2}}) \frac{f_{i,j+1} - f_{i,j}}{\Delta v_2},$$
(3.20)

in which we used the notations

$$\tilde{f}_{i+\frac{1}{2},j} = \left(1 - \delta_{i+\frac{1}{2},j}\right) f_{i+1,j} + \delta_{i+\frac{1}{2},j} f_{i,j},$$

and

$$\tilde{f}_{i,j+\frac{1}{2}} = \left(1 - \delta_{i,j+\frac{1}{2}}\right) f_{i,j+1} + \delta_{i,j+\frac{1}{2}} f_{i,j}.$$

The choice of the value of the coefficients  $\delta_{i+\frac{1}{2},j}$  and  $\delta_{i,j+\frac{1}{2}}$  is made in such a way that the stationary state structure is preserved (we refer to [37] for a detailed explanation on how this can be obtained). In particular, we set  $\mathcal{A}_{i+\frac{1}{2},j} = \mathcal{A}[f;\mathbf{u}](v_{1,i+\frac{1}{2}},v_{2,j},t)$  and

$$\delta_{i+\frac{1}{2},j} = \frac{1}{\lambda_{i+\frac{1}{2},j}} + \frac{1}{\exp\left\{\lambda_{i+\frac{1}{2},j}\right\}}, \text{ with } \lambda_{i+\frac{1}{2},j} = \frac{\Delta v_1 \left(\mathcal{A}_{i+\frac{1}{2},j} + \partial_{v_1} D_1(v_{i+\frac{1}{2},j})\right)}{D_1 \left(v_{i+\frac{1}{2},j}\right)},$$

then  $\mathcal{B}_{i,j+\frac{1}{2}} = \mathcal{B}[f; \mathbf{u}](v_{1,i}, v_{2,j+\frac{1}{2}}, t)$  and

$$\delta_{i,j+\frac{1}{2}} = \frac{1}{\lambda_{i,j+\frac{1}{2}}} + \frac{1}{\exp\left\{\lambda_{i,j+\frac{1}{2}}\right\}}, \text{ with } \lambda_{i,j+\frac{1}{2}} = \frac{\Delta v_2 \left(\mathcal{B}_{i,j+\frac{1}{2}} + \partial_{v_2} D_2(v_{i,j+\frac{1}{2}})\right)}{D_2(v_{i,j+\frac{1}{2}})},$$

a choice that guarantees second order accuracy in space. We now introduce the same time discretization used for the semi-Lagrangian scheme and use a second order in time discretization for the temporal derivatives appearing in (3.19). In particular, we use a second order implicit-explicit (IMEX) Runge-Kutta scheme defined as follows ([37, 15]). We formally duplicate the number of variables so that our problem becomes

$$\frac{\mathrm{d}}{\mathrm{d}t} f_{i,j}(t) = \mathcal{S}_{i,j}[\mathbf{f}, \mathbf{g}],$$

$$\frac{\mathrm{d}}{\mathrm{d}t} g_{i,j}(t) = \mathcal{S}_{i,j}[\mathbf{f}, \mathbf{g}],$$
(3.21)

where

$$S_{i,j}[\mathbf{f}, \mathbf{g}] = \frac{\mathcal{F}_{i+\frac{1}{2},j}^{(1)}[\mathbf{f}, \mathbf{g}](t) - \mathcal{F}_{i-\frac{1}{2},j}^{(1)}[\mathbf{f}, \mathbf{g}](t)}{\Delta v_1} + \frac{\mathcal{F}_{i,j+\frac{1}{2}}^{(2)}[\mathbf{f}, \mathbf{g}](t) - \mathcal{F}_{i,j-\frac{1}{2}}^{(2)}[\mathbf{f}, \mathbf{g}](t)}{\Delta v_2},$$

and

$$\mathcal{F}_{i+\frac{1}{2},j}^{(1)}[\mathbf{f},\mathbf{g}] = \mathcal{A}_{i+\frac{1}{2},j}[\mathbf{g}] \left( \left( 1 - \delta_{i+\frac{1}{2},j}[\mathbf{g}] \right) f_{i+1,j} + \delta_{i+\frac{1}{2},j}[\mathbf{g}] f_{i,j} \right) 
+ \frac{\sigma^{2}}{2} D_{1}(v_{i+\frac{1}{2},j}) \frac{f_{i+1,j} - f_{i,j}}{\Delta v_{1}}, 
\mathcal{F}_{i,j+\frac{1}{2}}^{(2)}[\mathbf{f},\mathbf{g}] = \mathcal{B}_{i,j+\frac{1}{2}}[\mathbf{g}] \left( \left( 1 - \delta_{i,j+\frac{1}{2}}[\mathbf{g}] \right) f_{i,j+1} + \delta_{i,j+\frac{1}{2}}[\mathbf{g}] f_{i,j} \right) 
+ \frac{\nu^{2}}{2} D_{2}(v_{i,j+\frac{1}{2}}) \frac{f_{i,j+1} - f_{i,j}}{\Delta v_{2}}.$$
(3.22)

where  $[\cdot]$  denotes functional dependence. Defining  $g_{i,j}^n=f_{i,j}^n$ , the implicit-explicit Runge-Kutta scheme can be written as

$$\begin{cases}
f_{i,j}^{n+1} = f_{i,j}^{n} + \Delta t \sum_{k=1}^{s} b_{k} \mathcal{S}_{i,j}[\mathbf{F}^{k}, \mathbf{G}^{k}], \\
g_{i,j}^{n+1} = f_{i,j}^{n} + \Delta t \sum_{k=1}^{s} \tilde{b}_{k} \mathcal{S}_{i,j}[\mathbf{F}^{k}, \mathbf{G}^{k}],
\end{cases}$$
(3.23)

where  $\mathbf{F}^h$  and  $\mathbf{G}^h$ ,  $h = 1, \dots, s$  are defined by

$$\begin{cases}
F_{i,j}^{h} = f_{i,j}^{n} + \Delta t \sum_{k=1}^{h} a_{hk} S_{i,j} [\mathbf{F}^{k}, \mathbf{G}^{k}], \\
G_{i,j}^{h} = f_{i,j}^{n} + \Delta t \sum_{k=1}^{h-1} \tilde{a}_{hk} S_{i,j} [\mathbf{F}^{k}, \mathbf{G}^{k}],
\end{cases}$$
(3.24)

for all h = 1, ..., s. In order to make the duplication of the system only apparent we set  $b_k = \tilde{b}_k$ , so  $f_{i,j}^{n+1} = g_{i,j}^{n+1}$ , and to obtain second order accuracy in time we set s = 2 and

$$a_{11} = 0$$
,  $a_{21} = a_{22} = \frac{1}{2}$ ,  $\tilde{a}_{21} = 1$ , and  $b_k = \tilde{b}_k = \frac{1}{2}$ ,  $k = 1, 2$ .

#### 4 Numerical simulations

In Section 4.1 and 4.2, given h the solution obtained with a numerical scheme, we compute the normalized  $L^2$  and  $L^{\infty}$  errors with respect to an exact (or reference) solution  $\hat{h}$ , defined as

$$E_2(h) = \frac{\|h - \hat{h}\|_2}{\|\hat{h}\|_2}, \quad E_{\infty}(h) = \frac{\|h - \hat{h}\|_{\infty}}{\|\hat{h}\|_{\infty}}.$$
 (4.25)

#### 4.1 Convergence to the stationary state for the Fokker-Planck

In this first simulation we show the second order convergence of the solution to the Fokker–Planck to its stationary state. The general expression of the steady state of (2.4) is not known, however under some restrictive assumptions it is possible to compute it. We put ourselves in the one dimensional setting,  $v \in \Omega = [-1, 1]$ , and we suppose that  $D(v) = \frac{\sigma^2}{2}(1 - v^2)^2$ , u(v, t) = 0, and  $P(v, v_*) = 1$  so that the nonlocal drift functional becomes

$$\mathcal{P}[f](v,t) = \alpha \left( \int_{\Omega} v_* f(v_*,t) \, dv_* - v \right) = \alpha \left( m_v(t) - v \right).$$

The Fokker-Planck equation (2.4) can then be rewritten as

$$\frac{\partial f}{\partial t} = -\alpha \frac{\partial ((m_v(t) - v)f)}{\partial v} + \frac{\sigma^2}{2} \frac{\partial^2 ((1 - v^2)^2 f)}{\partial v^2},\tag{4.26}$$

whose stationary solution  $f^{\infty}(v)$  is given by

$$f^{\infty}(v) = K_{\infty}(1+v)^{-2+\alpha \bar{m}_v/2\sigma^2} (1-v)^{-2-\alpha \bar{m}_v/2\sigma^2} \exp\left\{-\frac{\alpha(1-\bar{m}_v v)}{\sigma^2(1-v^2)}\right\},\,$$

where  $K_{\infty} > 0$  is such that

$$\int_{\Omega} f^{\infty}(v) \mathrm{d}v = 1$$

(we refer, for instance, to [39, 4] for more details in the computations). We focus on the convergence of the numerical solution to (4.26) using the scheme described in Section 3.2. Starting from an initial condition given by the uniform distribution in  $\Omega$ , we check the rate of convergence of our scheme to the analytical steady state with  $\alpha = 1$ ,  $\sigma^2 = 2 \times 10^{E-2}$ , and  $\Delta t = \Delta v/2$ . We compute the errors for several choices of the value of  $\Delta v$ , defined as  $|\Omega|/2^{N_v}$ , where  $2^{N_v}$  is the number of intervals in which the solution is approximated. Figure 4.1, on the left, shows the initial condition, the numerical solution at time t = 1, 2, 3 and the stationary state for  $N_v = 12$ , while on the right we have the  $L^2$  and  $L^\infty$  errors defined in (4.25) compared to the slope of the order 2. Table 4.1 reports the value of the errors for each choice of numbers of the intervals  $2^{N_v}$  used in the discretization of  $\Omega$ .

# 4.2 Order check with fixed suboptimal control for the Hamilton–Jacobi equation

Consider again the one dimensional setting. We want to simulate the solution to (2.10) with a fixed f and a suboptimal control, in order to check the second-order accuracy of the semi-Lagrangian

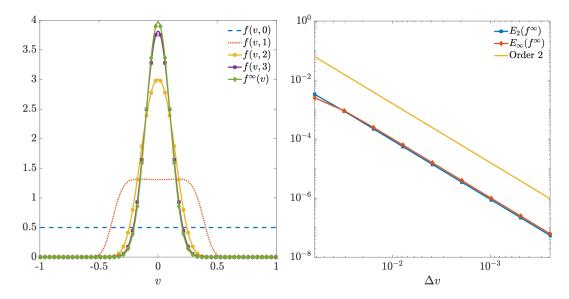


Figure 4.1: Time evolution of the numerical approximation of f(v,t) (left) and convergence to the stationary state (right). The direction of the horizontal axis is inverted in the second picture.

scheme with nonlocal drift and forcing term. First, we compute a reference solution on a spatial grid with  $N_v = 2^{13}$  discretization points solving

$$\begin{cases}
\partial_t f(v,t) = -\partial_v \left( \mathcal{P}[f](v,t) + u(v,t) \right) f + \partial_v^2 \left( D(v)f \right), & (v,t) \in \Omega \times (0,T] \\
f(v,0) = K_0 \exp\left( -(v-\lambda)^2/(2\rho^2) \right), & v \in \Omega \\
-\partial_t \psi = \left( \mathcal{P}[f](v,t) + u(v,t) \right) \partial_v \psi + D(v) \partial_{vv} \psi \\
+ \mathcal{Q}[f,\psi](v,t) + \frac{1}{2} \left( |v-\overline{v}|^2 s(c) + \gamma |u|^2 \right), & (v,t) \in \Omega \times [0,T), \\
\psi(v,0) = 0, & v \in \Omega,
\end{cases}$$
(4.27)

coupled with zero-flux boundary conditions for the Fokker–Planck equation and homogeneous Neumann boundary conditions for the Hamilton–Jacobi. We set  $\alpha=1$ ,  $P(v,v_*)=1$ , and h(v)=0 in (2.6), and set diffusion equal to  $D(v)=\sigma^2(1-v^2)^2/2$  with  $\sigma^2=10^{-2}$ . We choose final time T=1, and s(c)=1,  $\overline{v}=0.2$ ,  $\gamma=0.05$  in (2.10), and we fix as suboptimal control

$$u(v,t) = \left(-\frac{5}{2}v + \frac{1}{2}\right)(T-t).$$

The initial condition for the Fokker–Planck is given by

$$f_0(v) = K_0 e^{-\frac{(v+0.5)^2}{0.5}}$$

where the constant  $K_0 > 0$  is chosen so that

$$\int_{\Omega} f_0(v) \mathrm{d}v = 1.$$

Table 4.1: Errors and convergence rates for the Fokker–Planck equation at the stationary state. In all simulations  $\Delta t = \Delta v/2$ .

$\overline{N_v}$	$E_2(f^{\infty})$	$p_2$	$E_{\infty}(f^{\infty})$	$p_{\infty}$
4	$3.2925 \times 10^{-3}$	/	$2.5138 \times 10^{-3}$	/
5	$8.8520 \times 10^{-4}$	1.90	$9.1545 \times 10^{-4}$	1.46
6	$2.2177 \times 10^{-4}$	2.00	$2.4692 \times 10^{-4}$	1.89
7	$5.5473 \times 10^{-5}$	2.00	$6.2862 \times 10^{-5}$	1.97
8	$1.3870 \times 10^{-5}$	2.00	$1.5786 \times 10^{-5}$	1.99
9	$3.4676 \times 10^{-6}$	2.00	$3.9510 \times 10^{-6}$	2.00
10	$8.6691 \times 10^{-7}$	2.00	$9.8802 \times 10^{-7}$	2.00
11	$2.1673 \times 10^{-7}$	2.00	$2.4702 \times 10^{-7}$	2.00
12	$5.4182 \times 10^{-8}$	2.00	$6.1757 \times 10^{-8}$	2.00

Once we have the reference solution for both the Fokker–Planck and the Hamilton–Jacobi we use the reference  $f(v_1, v_2, t)$  as a datum and compute the errors for equation (2.10) at time t = 0. Table 4.2 report the errors as defined in (4.25) and confirm the order 2 in both norms. Figure 4.2, on the left, shows the approximation of the solution to the adjoint equation for t = 0, 0.25, 0.5, 0.75 and the terminal condition t = 1, while on right the second order convergence to the reference solution is shown.

Table 4.2: Errors and convergence orders for the Hamilton–Jacobi equation at the initial time t=0. In all simulations  $\Delta t = \Delta v$ .

$\overline{N_v}$	$E_2(\psi(\cdot,0))$	$p_2$	$E_{\infty}(\psi(\cdot,0))$	$p_{\infty}$
4	$8.8348 \times 10^{-2}$	/	$8.8453 \times 10^{-2}$	/
5	$2.1201 \times 10^{-2}$	2.05	$2.0812 \times 10^{-2}$	2.09
6	$4.8843 \times 10^{-3}$	2.12	$5.0052 \times 10^{-3}$	2.06
7	$1.1746 \times 10^{-3}$	2.06	$1.2131 \times 10^{-3}$	2.04
8	$2.8294 \times 10^{-4}$	2.05	$2.9106 \times 10^{-4}$	2.06
9	$6.6038 \times 10^{-5}$	2.10	$6.7338 \times 10^{-5}$	2.11
10	$1.4541 \times 10^{-5}$	2.18	$1.4293 \times 10^{-5}$	2.24
11	$3.1253 \times 10^{-6}$	2.22	$2.4059 \times 10^{-6}$	2.57
12	$9.2072 \times 10^{-7}$	1.76	$6.8016 \times 10^{-7}$	1.82

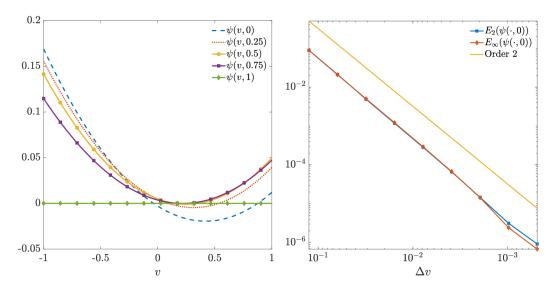


Figure 4.2: Time evolution of the numerical approximation of  $\psi(v,t)$  (left) and convergence to the reference solution (right). The direction of the horizontal axis is inverted in the second picture.

#### 4.3 Numerical experiments in social dynamics

This concluding section is dedicated to two qualitative simulations in two spatial dimensions. In the first one, to which is dedicated Section 4.3.1, the first spatial variable has to be intended as the opinion variable, while the second one represents the number of social media contacts of the agents in a population. The simulation shows how an external action on the opinions of certain groups of people can have a high impact in shaping the general sentiment of the entire population. In Section 4.3.2, instead, the two variables  $v_1$  and  $v_2$  represent two opinions on different topics, one influencing the evolution of the other and vice versa. We show how an external force can modify the evolution of the general idea of the public and lead to consensus on an objective combination of opinions, even when the uncontrolled case offers a completely different outcome.

#### 4.3.1 Evolving opinions and social media contacts

In this simulation we suppose that  $\Omega_1 = [-1, 1]$ , while  $\Omega_2 = [1, v_{2,M}]$  with  $v_{2,M} = 40$ . Heuristically, we can consider the first variable  $v_1$  to be the population opinion on a matter and the second one  $v_2$  to be the number of social media contacts. Following the construction in [4] we choose in (2.6)  $h_1(v_1, v_2) = 0$ ,  $\alpha_1 = 1$ ,

$$P(v_1, v_2, v_1^*, v_2^*) = \chi \left( |v_1 - v_1^*| \le \Delta \frac{v_2^*}{v_2 + v_2^*} \right) \frac{v_2^*}{v_2 + v_2^*},$$

 $P_2(v_1, v_2, v_1^*, v_2^*) = 0, u_2(v_1, v_2, t) = 0,$ and

$$h_2(v_1, v_2) = \frac{\mu}{2} \log \left(\frac{v_2}{\hat{v}_2}\right) v_2,$$
 (4.28)

where we set  $\mu = 0.1$  and  $\hat{v}_2 = 20$ , and diffusion matrix

$$\begin{bmatrix} \frac{\sigma^2}{2} \left( 1 - v_1^2 \right) & 0\\ 0 & \frac{\nu^2}{2} v_2^2 \end{bmatrix},$$

with  $\Delta = 2$ ,  $\sigma^2 = \nu^2 = 2 \times 10^{-3}$ . Notice that this choice of  $\mathcal{G}[f; \mathbf{u}](v_1, v_2, t)$  leads to  $\mathcal{Q}_2[f](v_1, v_2, t) = 0$  in (2.10). The initial condition is the sum of three bivariate gaussians

$$\begin{split} f_0(v_1,v_2) &= K_0 \left( e^{-\frac{1}{2(1-0.5^2)} \left( \frac{(v_1+0.5).^2}{0.01} + \left( \frac{v_1+0.5}{0.1} \right) \left( \frac{v_2-10}{5} \right) + \frac{(v_2-10)^2}{25} \right)} \right. \\ &+ e^{-\frac{1}{2(1-0.5^2)} \left( \frac{(v_1-0.75)^2}{0.01} - \left( \frac{v_1-0.75}{0.1} \right) \left( \frac{v_2-50}{5} \right) + \frac{(v_2-50)^2}{25} \right)} \\ &+ e^{-\frac{1}{2(1-0.75^2)} \left( \frac{(v_1+0.75)^2}{0.01} - 1.5 \left( \frac{v_1+0.75}{0.1} \right) \left( \frac{v_2-50}{5} \right) + \frac{(v_2-50)^2}{25} \right)} \right), \end{split}$$

The constant  $K_0$  normalizes the initial total mass, i.e.

$$\int_{-1}^{1} \int_{1}^{v_{2,M}} f_0(v_1, v_2) dv_1 dv_2 = 1.$$

We fix the final time T=3. Figure 4.3 shows the initial condition  $f_0$  (left), the numerical approximation of the uncontrolled density at time t=1.5 (center) and t=3 (right). With this choice of interaction function and in the absence of control, the density tends to concentrate mainly around two negative opinions. In the functional (2.8) we choose  $\bar{v}_1=0.3$  and  $\gamma=0.05$ . We fix

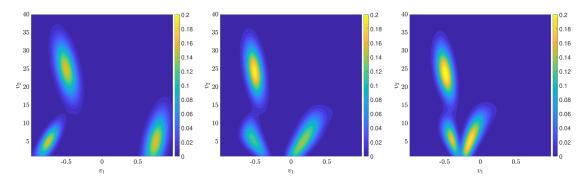


Figure 4.3: Uncontrolled density  $f(\mathbf{v},t)$  at time T=0 (left), t=1.5 (center), and t=3 (right).

 $s_2(v_1, v_2) = 0$  and we perform simulations for two different values of the function  $s_1(v_1, v_2)$ : in the first case

$$s_1(v_1, v_2) = \frac{1}{1 + e^{-\frac{1}{2}(\hat{v}_2 - v_2)}},\tag{4.29}$$

meaning that the control acts mainly on the agents with less than  $\hat{v}_2$  contacts, while in the second case we set

$$s_1(v_1, v_2) = \frac{1}{1 + e^{-\frac{1}{2}(v_2 - \hat{v}_2)}},\tag{4.30}$$

so the control acts more intensely on agents with more than  $\hat{v}_2$  contacts. Figure 4.4 shows a comparison between the controlled density (upper row) and the control function (bottom row) at time t=0 (left), t=1.5 (center) and t=3 (right) for the choice in (4.29). We can see how the control tends to concentrate the agents with a lower number of contacts around  $v_1=0.3$ , as expected, but part of the influent population (with a higher value of  $v_2$ ) stays on the negative half of  $\Omega_1$ . Figure 4.6 shows a comparison between the controlled density (upper row) and the control function (bottom row) at time t=0 (left), t=1.5 (center) and t=3 (right) for the choice in (4.30). Again, we see how the control is able to concentrate the density around  $v_1=0.3$ , acting primarily on the part of the population with a higher number of contacts. Due to the expression of the interaction function P, also the segment of the population with less contacts gets influenced and modifies its opinion, ending up with a positive value of  $v_1$ . Figure 4.6 shows, instead, the value of the cost functional  $\mathcal{J}(\mathbf{u}^{(k)}; f_0)$  for the various iterations k of the gradient descent method compared to the computed optimal value  $\mathcal{J}(\mathbf{u}^*; f_0)$ , both for the choice of  $s_1$  in (4.29) (left) and in (4.30) (right).

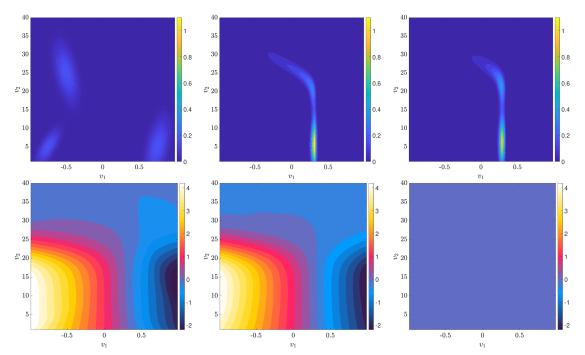


Figure 4.4: Case with  $s_1(v_1, v_2)$  as in (4.29). Contour plots of the density  $f(\mathbf{v}, t)$  (upper row), and the control  $\mathbf{u}(\mathbf{v}, t)$  (bottom row) for time t = 0 (left), t = 1.5 (center) and t = 3 (right).

#### 4.3.2 Bivariate opinion model

In this last Section we assume that  $\Omega_1 = \Omega_2 = [-1, 1]$  and the two variables can be interpreted as two opinions. In (2.6) we set  $h_1(v_1, v_2) = h_2(v_1, v_2) = 0$ , while for the nonlocal part of the drift

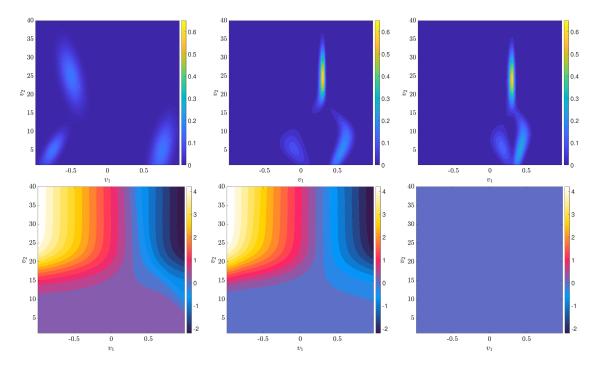


Figure 4.5: Case with  $s_1(v_1, v_2)$  as in (4.30). Contour plots of the density  $f(\mathbf{v}, t)$  (upper row), and the control  $\mathbf{u}(\mathbf{v}, t)$  (bottom row) at time t = 0 (left), t = 1.5 (center) and t = 3 (right).

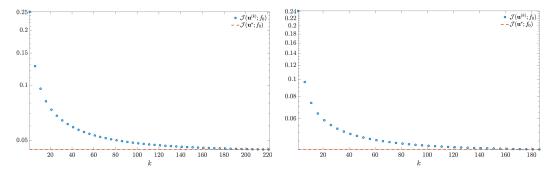


Figure 4.6: Value of the cost functional  $\mathcal{J}(\mathbf{u}^{(k)}; f_0)$  at each iteration k compared to the computed optimal value  $\mathcal{J}(\mathbf{u}^*; f_0)$  for (4.29) (left), and (4.30) (right).

we choose  $\alpha_1 = \alpha_2 = 1$ ,

$$P_1(v_1, v_2, v_1^*, v_2^*) = P_2(v_1, v_2, v_1^*, v_2^*) = \sqrt{(v_1 - v_1^*)^2 + (v_2 - v_2^*)^2} \le \Delta, \tag{4.31}$$

with  $\Delta = 1$ . We set as diffusion matrix

$$\mathcal{D}(v_1, v_2) = \begin{bmatrix} \frac{\sigma^2}{2} (1 - v_1^2)(1 - v_2^2) & 0\\ 0 & \frac{\nu^2}{2} (1 - v_1^2)(1 - v_2^2) \end{bmatrix},$$

with  $\sigma^2 = \nu^2 = 2 \times 10^{-2}$ . We fix final time T = 2, and in (2.8) we set  $\overline{v}_1 = \overline{v}_2 = 0.6$ , and  $\gamma = 0.05$ . We start from a polarized initial condition given by

$$\begin{split} f_0(v_1,v_2) &= e^{-\frac{1}{2(1-0.5^2)} \left( \frac{(v_1+0.5)^2}{0.01} + \left( \frac{v_1+0.5}{0.1} \right) \left( \frac{v_2-0.5}{0.1} \right) + \frac{(v_2-0.5)^2}{0.01} \right)} \\ &+ e^{-\frac{1}{2(1-0.5^2} \left( \frac{(v_1-0.5)^2}{0.01} + \left( \frac{v_1-0.5}{0.1} \right) \left( \frac{v_2+0.5}{0.1} \right) + \frac{(v_2+0.5)^2}{0.01} \right)}. \end{split}$$

meaning that the initial density consists of two separated clusters of opinions. Figures 4.7 shows a comparison between the initial condition (left), the uncontrolled density at time t=1 (center) and the uncontrolled density at the final time t=2 (right). We can see how, with our choice of parameters, the uncontrolled setting leads to a consensus around zero both for the first and the second variable. Figure 4.8 shows a comparison between the controlled density and the control at time t=0 (left), t=1 (center) and t=2 (right). We can see how the controlled density concentrates around the target  $(\bar{v}_1, \bar{v}_2)$  and that the control points towards this point (and is then equal to zero at the final time t=2). Figure 4.9 shows the value of the cost functional  $\mathcal{J}(\mathbf{u}^{(k)}; f_0)$  for the various iterations k of the gradient descent method compared to the final computed optimal value  $\mathcal{J}(\mathbf{u}^*; f_0)$ .

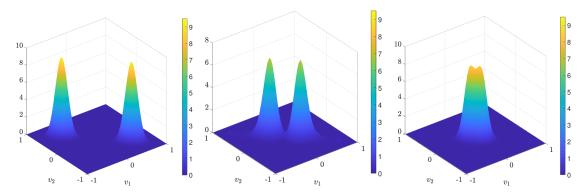


Figure 4.7: The initial condition  $f(\mathbf{v}, 0)$  (left), the uncontrolled density at time t = 1 (center) and at time t = 2 (right).

#### 5 Conclusions

In this work, we introduced a second-order numerical scheme for solving optimal control problems constrained by nonlinear Fokker–Planck equations, with applications in socio-economic dynamics and opinion formation. The control problem was formulated using the Lagrange multiplier approach, leading to a coupled forward-backward system consisting of a Fokker–Planck equation modeling socio-economic phenomena and a Hamilton–Jacobi–Bellman equation for the adjoint variable. To achieve high accuracy and stability, we employed an asymptotic preserving scheme for the forward equation and a semi-Lagrangian scheme for the backward equation, allowing for large time steps without the restrictive CFL condition. The coupling between the two equations was resolved via a reduced-gradient optimization strategy. Numerical experiments confirmed the

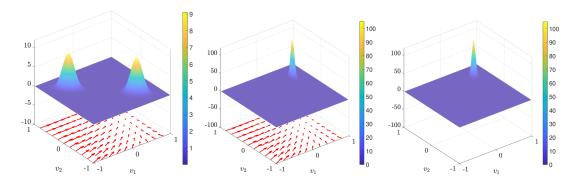


Figure 4.8: Comparison between the density  $f(\mathbf{v},t)$  (as surface plot) and the optimal control  $\mathbf{u}^*(\mathbf{v},t)$  (red arrows) at time t=0 (left), t=1 (center) and t=2 (right).

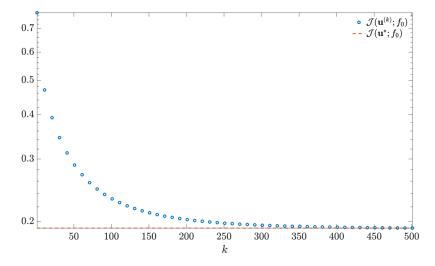


Figure 4.9: Value of the cost functional  $\mathcal{J}(\mathbf{u}^{(k)}; f_0)$  at each iteration k of the gradient descent algorithm compared to the final optimal value  $\mathcal{J}(\mathbf{u}^*; f_0)$ .

second-order accuracy of the scheme and demonstrated its effectiveness in controlling opinion dynamics under various settings, including evolving social networks and multi-dimensional cases.

Future research directions include the study of Fokker-Planck models in the presence of uncertainties that require the design of robust controls with respect to certain risk measures, and with localized action of the control. A further direction is to investigate the development of numerical schemes able to cope efficiently with the optimal control of partial differential models in presence of multiple scale, this models are of paramount importance in applications where heterogeneous dynamics are involved, such as opinion dynamics coupled with epidemics, or crowd dynamics with emotional contagion.

## Acknowledgments

This work has been written within the activities of the GNCS group of INdAM. GA and EC thanks the support of MUR-PRIN Project 2022 PNRR No. P2022JC95T, "Data-driven discovery and control of multi-scale interacting artificial agent systems", and GA also of MUR-PRIN Project 2022 No. 2022N9BM3N "Efficient numerical schemes and optimal control methods for time-dependent partial differential equations" both financed by the European Union - Next Generation EU.

## References

- [1] M. Aduamoah, B. D. Goddard, J. W. Pearson, and J. C. Roden. Pseudospectral methods and iterative solvers for optimization problems from multiscale particle dynamics. *BIT Numerical Mathematics*, 62:1703–1743, 2022.
- [2] G. Albi, S. Bicego, and D. Kalise. Control of high-dimensional collective dynamics by deep neural feedback laws and kinetic modelling. arXiv preprint arXiv:2404.02825, 2024.
- [3] G. Albi, M. Caliari, E. Calzola, and F. Cassini. Exponential integrators for a mean-field selective optimal control problem. *Journal of Approximation Software*, 1(2), 2024.
- [4] G. Albi, E. Calzola, and G. Dimarco. A data-driven kinetic model for opinion dynamics with social network contacts. *European Journal of Applied Mathematics*, pages 1–27, 2024.
- [5] G. Albi, Y.-P. Choi, M. Fornasier, and D. Kalise. Mean field control hierarchy. *Appl. Math. Optim.*, 76(1):93–135, 2017.
- [6] G. Albi, G. Dimarco, F. Ferrarese, and L. Pareschi. Instantaneous control strategies for magnetically confined fusion plasma. *Journal of Computational Physics*, page 113804, 2025.
- [7] G. Albi, L. Pareschi, and M. Zanella. Boltzmann-type control of opinion consensus through leaders. *Philosophical Transactions of the Royal Society A: Mathematical, Physical and Engineering Sciences*, 372(2028):20140138, 2014.
- [8] A. Alla, M. Falcone, and D. Kalise. An efficient policy iteration algorithm for dynamic programming equations. SIAM Journal on Scientific Computing, 37(1):A181–A200, 2015.
- [9] A. Alla, D. Kalise, and V. Simoncini. State-dependent riccati equation feedback stabilization for nonlinear pdes. *Advances in Computational Mathematics*, 49(1):9, 2023.
- [10] M. Annunziato and A. Borzì. A Fokker-Planck control framework for multidimensional stochastic processes. *Journal of Computational and Applied Mathematics*, 237(1):487–507, 2013.
- [11] M. Aronna and F. Tröltzsch. First and second order optimality conditions for the control of Fokker-Planck equations. *Esaim control Optimisation and Calculus of Variations*, 27:15, 2021.
- [12] S. Bicego, D. Kalise, and G. A. Pavliotis. Computation and control of unstable steady states for mean field multiagent systems. arXiv preprint arXiv:2406.11725, 2024.

- [13] A. Bobylev and K. Nanbu. Theory of collision algorithms for gases and plasmas based on the Boltzmann equation and the landau-Fokker-Planck equation. *Physical Review E*, 61(4):4576, 2000.
- [14] L. Bonaventura, E. Calzola, E. Carlini, and R. Ferretti. Second order fully semi-Lagrangian discretizations of advection-diffusion-reaction systems. J. Sci. Comput., 88(1):Paper No. 23, 29, 2021.
- [15] S. Boscarino, F. Filbet, and G. Russo. High order semi-implicit schemes for time dependent partial differential equations. *J. Sci. Comput.*, 68(3):975–1001, 2016.
- [16] T. Breiten and K. Kunisch. Optimal control of a nonlinear kinetic Fokker-Planck equation. arXiv preprint arXiv:2501.03784, 2025.
- [17] T. Breiten, K. Kunisch, and L. Pfeiffer. Control strategies for the Fokker-Planck equation. ESAIM: Control, Optimisation and Calculus of Variations, 24(2):741–763, 2018.
- [18] T. Breitenbach and A. Borzì. The Pontryagin maximum principle for solving Fokker–Planck optimal control problems. *Computational Optimization and Applications*, 76(2):499–533, 2020.
- [19] M. Burger, R. Pinnau, C. Totzeck, and O. Tse. Mean-field optimal control and optimality conditions in the space of probability measures. *SIAM J. Control Optim.*, 59(2):977–1006, 2021.
- [20] S. Cacace and R. Ferretti. Efficient implementation of characteristic-based schemes on unstructured triangular grids. *Comput. Appl. Math.*, 41(1):Paper No. 19, 24, 2022.
- [21] E. Calzola, E. Carlini, X. Dupuis, and F. J. Silva. A semi-Lagrangian scheme for Hamilton-Jacobi-Bellman equations with oblique derivatives boundary conditions. *Numer. Math.*, 153(1):49–84, 2023.
- [22] J. A. Carrillo, Y.-P. Choi, C. Totzeck, and O. Tse. An analytical framework for consensus-based global optimization method. *Mathematical Models and Methods in Applied Sciences*, 28(06):1037–1066, 2018.
- [23] J. A. Carrillo, R. Eftimie, and F. Hoffmann. Non-local kinetic and macroscopic models for self-organised animal aggregations. *Kinetic and Related Models*, 8(3):413–441, 2015.
- [24] J. Chang and G. Cooper. A practical difference scheme for Fokker-Planck equations. *Journal of Computational Physics*, 6(1):1–16, 1970.
- [25] P. Degond, M. Herda, and S. Mirrahimi. A Fokker-Planck approach to the study of robustness in gene expression. *Mathematical Biosciences and Engineering*, 17(6):6459–6486, 2020.
- [26] G. Dimarco and G. Toscani. Social climbing and Amoroso distribution. *Mathematical Models and Methods in Applied Sciences*, 30(11):2229–2262, 2020.
- [27] M. Falcone and R. Ferretti. Semi-Lagrangian schemes for Hamilton-Jacobi equations, discrete representation formulae and Godunov methods. *J. Comput. Phys.*, 175(2):559–575, 2002.
- [28] R. Ferretti. A technique for high-order treatment of diffusion terms in semi-Lagrangian schemes. Communications in Computational Physics, 8(2):445–470, 2010.

- [29] A. Fleig and R. Guglielmi. Optimal control of the Fokker-Planck equation with space-dependent controls. *Journal of Optimization Theory and Applications*, 174:408–427, 2017.
- [30] M. Fornasier, H. Huang, L. Pareschi, and P. Sünnen. Consensus-based optimization on hypersurfaces: Well-posedness and mean-field limit. *Mathematical Models and Methods in Applied Sciences*, 30(14):2725–2751, 2020.
- [31] M. Fornasier, B. Piccoli, and F. Rossi. Mean-field sparse optimal control. *Philosophi-cal Transactions of the Royal Society A: Mathematical, Physical and Engineering Sciences*, 372(2028):20130400, 2014.
- [32] J. Franceschi, A. Medaglia, and M. Zanella. On the optimal control of kinetic epidemic models with uncertain social features. Optimal Control Applications and Methods, 45(2):494–522, 2024.
- [33] M. Gugat, M. Herty, and C. Segala. The turnpike property for mean-field optimal control problems. *European Journal of Applied Mathematics*, 35(6):733–747, 2024.
- [34] J.-L. Lions. Optimal control of systems governed by partial differential equations, volume Band 170 of Die Grundlehren der mathematischen Wissenschaften. Springer, Berlin, Heidelberg, 1971. Translated from the French by S. K. Mitter.
- [35] M. Mohammadi and A. Borzì. Analysis of the Chang–Cooper discretization scheme for a class of Fokker–Planck equations. *Journal of Numerical Mathematics*, 23(3):271–288, 2015.
- [36] L. Pareschi and G. Toscani. Wealth distribution and collective knowledge: a Boltzmann approach. *Philosophical Transactions of the Royal Society A: Mathematical, Physical and Engineering Sciences*, 372(2028):20130396, 2014.
- [37] L. Pareschi and M. Zanella. Structure preserving schemes for nonlinear Fokker-Planck equations and applications. *J. Sci. Comput.*, 74(3):1575–1600, 2018.
- [38] A. Quarteroni. Numerical models for differential problems, volume 16 of Modeling, Simulation & Applications. Springer, Milan, second edition, 2014.
- [39] G. Toscani. Kinetic models of opinion formation. Communications in mathematical sciences, 4(3):481–496, 2006.